Available online at www.sciencedirect.com

SciVerse ScienceDirect

Ceramics International 39 (2013) 6899–6905

CERAMICS INTERNATIONAL

www.elsevier.com/locate/ceramint

Preparation of nano-sized $Mg_{0.6}Al_{0.8}Ti_{1.6}O_5$ powders using the inorganic salts route

M. Sobhani*, A. Sedaghat, T. Ebadzadeh, M. Ebrahimi

Ceramic Department of Materials and Energy Research Center, Alborz, Iran

Received 26 January 2013; received in revised form 11 February 2013; accepted 11 February 2013
Available online 17 February 2013

Abstract

Stable magnesium aluminum titanate ceramics ($Mg_{0.6}Al_{0.8}Ti_{1.6}O_5$) compound has been successfully synthesized with a straightforward non-hydrolytic sol–gel process using an inorganic metal compound as cation source supplier at about 600 °C. The raw materials $MgCl_2 \cdot 2H_2O$, $AlCl_3$, $TiCl_4$, and citric acid were dissolved in ethanol. Prepared gel was dried at 120 °C and calcined at various temperatures in an electric furnace. The results of X-ray diffraction (XRD) and simultaneous thermal analysis (STA) demonstrate that the direct crystallization of mono-phase magnesium aluminum titanate from fluffy precursor at a temperature below aluminum titanate decomposition temperature range is feasible. Field emission scanning electron microscopy (FESEM) and Brunauer–Emmett–Teller (BET) analysis show the nano-metric size of particles. The particle size and specific surface area of the powders varied from 16.5 to 27.6 nm and from 98.2 to 58.7 $m^2\,g^{-1}$ according to calcination temperatures (600 and 700 °C), respectively. The nano-particles had a strong tendency to agglomerate and were partially sintered at 1100 °C.

Keywords: A. Sol–gel; D. Aluminum titanate; Nano-particles; Non-hydrolytic

1. Introduction

Aluminum titanate or tialite (Al_2TiO_5) ceramics show several individual thermal properties and are suitable for different applications. It has an orthorhombic unit-cell in the Cmcm space-group with different thermal expansion coefficients (TECs) along normal crystallographic axes ($\alpha_a = 10.9 \times 10^{-6}\,K^{-1}$, $\alpha_b = 20.5 \times 10^{-6}\,K^{-1}$, $\alpha_c = 2.7 \times 10^{-6}\,K^{-1}$) [1,2]. The oxygen octahedral surrounds the metal ions; thereof both Al^{3+} and Ti^{4+} have a coordination number of 6 [2,3]. Polycrystalline aluminum titanate bodies show a very low TEC (α is about $(0.2–1.0) \times 10^{-6}\,°C^{-1}$) as a result of anisotropic expansion of such orthorhombic structure [4]. These properties make it suitable for high thermal shock resistance applications such as insulation of engine parts and in aluminum casting industries and automotive industries [5]. Formation of tialite proceeds with the following reaction at over eutectoid temperature of 1280 °C that has been experimentally confirmed by several authors [6,7]:

$$Al_2O_3(\alpha) + TiO_2(\text{rutile}) \rightarrow Al_2TiO_5(\beta), \quad \Delta G^o = 17{,}000 - 10.95\,T(\text{J/mol}) \tag{1}$$

The major problems associated with application of aluminum titanate is decomposition to Al_2O_3 and TiO_2 oxides during heat treatment (in the range of 900–1280 °C), with a maximum rate at about 1100 °C and low mechanical properties [8,9]. The mechanism of decomposition phenomena may be ascribed to the abnormal contraction behavior of lattice constant c during increment of temperature that caused an increase in distortion of crystal structure [2,10]. The effect of MgO and Fe_2O_3 additives on the prevention of the decomposition of tialite has been reported previously [5,11,12]. Also these additive oxides change the formation temperature of solid solution reaction of tialite [6,10]. As mentioned above, the transformation temperature of pure tialite is thermodynamically about 1280 °C while this temperature decreases in the presence of MgO due to the formation of magnesium aluminum titanate solid solution with $Mg_xAl_{2(1-x)}Ti_{(1+x)}O_5$ formula. When $x = 0.6$, there is no reported data for

*Corresponding author. Tel.: +98 9155022379; fax: +98 2636204139.
E-mail address: manoochehrsobhani@gmail.com (M. Sobhani).

0272-8842/$ - see front matter © 2013 Elsevier Ltd and Techna Group S.r.l. All rights reserved.
http://dx.doi.org/10.1016/j.ceramint.2013.02.024

decomposition of $Mg_{0.6}Al_{0.8}Ti_{1.6}O_5$ during heat treatment at about 1100 °C. Therefore, this composition can be introduced as a proper stabilized compound of tialite [3,10]. Preparation of aluminum titanate powder via other chemical reactions such as combustion and sol–gel techniques have been investigated [9,12]. In the sol–gel method there are two main schedules during the process, hydrolytic and non-hydrolytic sol–gel (NHSG) techniques [8,12]. In attention to the scientific reports on hydrolytic sol–gel, phase crystallization of aluminum titanate occurs above 1280 °C [8]. The procedure is carried out by hydrolysis and polymerization reactions of dissolved metal alkoxide in ethanol. TiO_2 and Al_2O_3 phases were observed during the calcination of dried gels at 700 and 1000 °C, respectively. Low temperature crystallization of tialite phase has been obtained through NHSG process [3,12,13]. Additionally, Innocenzi et al. [12] have successfully extended the low temperature sol–gel synthesis to the preparation of aluminum titanate films via repetitive dip-coating on silicon wafers. Inevitably, formation of other excess phases of TiO_2 such as rutile and anatase or α-alumina beside aluminum titanate phase, below 1280 °C is observed [12,14–16]. As reported [14] when toluene was used as a medium for metal alkoxides, the formation of $Mg_{0.6}Al_{0.8}$-$Ti_{1.6}O_5$ occurred above 1200 °C and unpleasant phases were formed. Therefore, the objective of present work is providing a straightforward sol–gel process to obtain an ideal mono-phase of magnesium aluminum titanate ($Mg_{0.6}Al_{0.8}Ti_{1.6}O_5$) with high purity. In comparison with other works in this area [12–14] the temperature of phase crystallization has been reduced with minimum content of other superfluous phases.

2. Experimental procedures

2.1. Materials and method

$MgCl_2 \cdot 2H_2O$, $AlCl_3$, $TiCl_4$, anhydride citric acid and absolute ethanol were used as raw materials and all were purchased from Merck Co. The sol–gel process was the synthesis route of the final products [15] with the use of inorganic salts. The molar ratio of Mg:Al and Ti:Al was 0.75:1 and 2:1, respectively, according to $Mg_{0.6}Al_{0.8}Ti_{1.6}O_5$ formula. Therefore, 2.89 g ($\approx$22 mmol) $MgCl_2 \cdot 2H_2O$, 3.92 g $AlCl_3$ ($\approx$29.4 mmol) and 6.45 cm^3 ($\approx$58.7 mmol) $TiCl_4$ were added to 100 cm^3 ethanol in an Erlenmeyer flask under magnetic stirring. Since the molar fraction of citric acid to all metallic cations was selected as 1:3, 7.05 g ($\approx$36 mmol) citric acid was introduced in the sol. It should be noted that a large amount of HCl gas would be exhausted during mixing process of metallic chlorides in ethanol (specifically for $TiCl_4$). Thus, to avoid the risk of explosion, the experimental process was carried out by the ventilation system. Thereafter, the excess ethanol was vaporized by stirring continuously at 80 °C for 4 h. The obtained sol was aged at room temperature for 12 h and reheated again at 80 °C to form a transparent concentrated pea-green gel. This gel was dried in an oven at 120 °C for 10 h to obtain a fluffy precursor. This precursor was easily crumbled and calcined at 600, 700, 800, and 1100 °C with a heating rate of 10 °C/min and soaking time of 2 h in an electrical furnace to obtain final ceramic powders.

2.2. Characterization methods and devices

The phase composition of powders after thermal treatment was determined by an X-ray diffractometer (Model: Siemens D-500) using CuK_α (λ=1.54 Å) radiation. The apparent crystallite size of $Mg_{0.6}Al_{0.8}Ti_{1.6}O_5$ powder was measured by the Scherrer equation

$$D = \frac{k\lambda}{\mathrm{Cos}\ \theta\ B(2\theta)} \tag{2}$$

where D is the apparent crystallite size, k is constant, λ is the wavelength, θ is the Bragg angle and $B(2\theta)$ is modified full-width at half-maximum (FWHM) in the diffraction line. To avoid the instrumental broadening, $B(2\theta)$ was adjusted using the following formula:

$$B(2\theta) = \sqrt{B_o^2(2\theta) - B_s^2} \tag{3}$$

where B_o is FWHM of the diffraction line that was determined by X'Pert HighScore software program. B_s is FWHM of the standard sample (silicon) diffraction lines.

Simultaneous thermal analysis (STA) with differential thermal analysis (DTA) and thermo-gravimetric (TG) curves was carried out in a PLSTA 1640 thermal analysis system in air atmosphere with a temperature-rising rate of 6 °C/min.

The specific surface area of calcined powders was measured via the Brunauer–Emmett–Teller (BET) method with nitrogen gas adsorption, using a surface area analyzer (Model: BELSORP II). Prior to the measurement of nitrogen adsorption, samples were outgassed under vacuum at 150 °C for 2 h. The equivalent spherical diameter (ESD or D) of the powders in nanometer dimension was calculated from the BET results using the following Equation [3]:

$$D = \frac{6000}{\rho_{powder}\ \mathrm{SSA}} \tag{4}$$

where ρ_{powder} is the density of the particle (assumed to be 3.7 g/cm^3) and SSA is the specific surface area of the powders (m^2/g).

A TESCAN field emission scanning electron microscope (FESEM, model MIRA II) was used to observe the microstructure of synthesized powders. The powders were dispersed into acetin using a laboratory ultrasonic device; the resultant suspensions were spread and dried on the surface of a sample holder and coated with gold to prevent from electron charge.

In order to examine the characteristics of the as-dried gel and calcined powders, Fourier transform infrared (FTIR) spectra of the samples were recorded in the wave number

range 4000–400 cm^{-1} at resolution of 4 cm^{-1} by a Shimadzu-FTIR spectrophotometer.

3. Results and discussions

In a non-hydrolytic sol–gel process the reaction of metallic chlorides with ethanol causes the formation of chloroalkoxide compounds and hydrochloric acid as a result of the following chemical reaction [3,17]:

$$MCl_n + xC_2H_5OH \rightarrow M(-OC_2H_5)_xCl_{n-x} + xHCl, \quad (M = Ti,\ Al) \tag{5}$$

Furthermore, an undesirable reaction between alcohols and hydrochloric acid leads to generation of alkyl halide and water, which brings about the hydrolysis of chloroalkoxides to form metal hydroxides. The above reaction processes can be described as follows [3,17]:

$$HCl + ROH \rightarrow RCl + H_2O \tag{6}$$

$$M(-OR)_xCl_{n-x} + nH_2O \rightarrow nM(OH)_n + (n-x)HCl + xROH \tag{7}$$

Fortunately while alkyl group (R) is ethyl, the reactions (6) and (7) do not occur due to low reactivity of ethanol [3]. The formation of a homogenous gel cannot occur easily because of reactions (6) and (7), as the phase segregation of metallic cations due to the separation of oxygen bonds leads to the formation of $M(OH)_n$ instead of desirable M–O–M' chains. These phenomena have been observed during the hydrolytic sol–gel process that finally cause the formation of TiO_2 (anatase or rutile) and α-Al_2O_3 phases. The STA curve of dried gel is presented in Fig. 1. The TG branch shows an undulatory slope shape from beginning to 570 °C as a result of stepwise weight reduction of the precursor during dehydration, oxidization and decomposition [15,18]. There is no more obvious occurrence from 570 °C to 1200 °C for both TG and DTA curves. The DTA branch presents a primary broadened endothermic curve before 270 °C that corresponds to vaporization of excess alcohols and HCl, and finally shows two main exothermic events [17]. The first event is upheaval exothermic variation in DTA curve that occurs at about 270 °C due to the initial decomposition of inorganic compound on reaction with oxygen. The second sharp exothermic peak expanded from 370 to 570 °C in DTA and the sharp slope in TG curves can be attributed to the combustion of residual carbonaceous components such as citrate base molecule, and the crystallization of ideal magnesium aluminum titanate phase. Overlapping of simultaneous events in DTA curve can be confirmed by considering X-ray patterns and TG curve which is another evidence of full homogeneity of precursor at atomic level.

Fig. 2 corresponds to the FTIR spectra of dried and calcined gels. The solid and dashed curves represent a gel dried at 120 °C in an oven and a prior gel calcined at 800 °C, respectively. Both curves exhibit bands at 3394–3431 and 1630–1635 cm^{-1}. These bands that represent stretching and bending vibrations modes of –OH groups, correspondingly [17], were smoothed by increasing thermal treatment temperature from 120 to 800 °C. Obviously, these vibrations in solid curve spectra are caused by M–O–H (M = Al, Ti, Mg) group in gel. In addition, the presence of –OH groups can be attributed to trace amount of the H_2O molecules unavoidably adsorbed onto the surface of the samples during analysis [19]. The C–O bonds in the citric acid molecule show a characteristic vibration in the range of 1700–1720 cm^{-1},while this characteristic vibration is not observed in the dried gel spectra (solid curve) at 120 °C. The carbon–oxygen double bond disappeared in FTIR spectra during the combination of the oxygen atoms with metallic cations (Al, Ti and Mg) to provide their coordinate number [19,20]. Other vibrations of dried gel spectra at 1402, 1230 and 1076 cm^{-1} can be attributed to C–H bending, C–O (for citric acid) stretch and C–O (for ethanol) stretch vibrations, respectively [17,20,21].

From synthesized powder spectra (dashed curve) the transmittance peaks at 509 and 680 cm^{-1} are assigned to

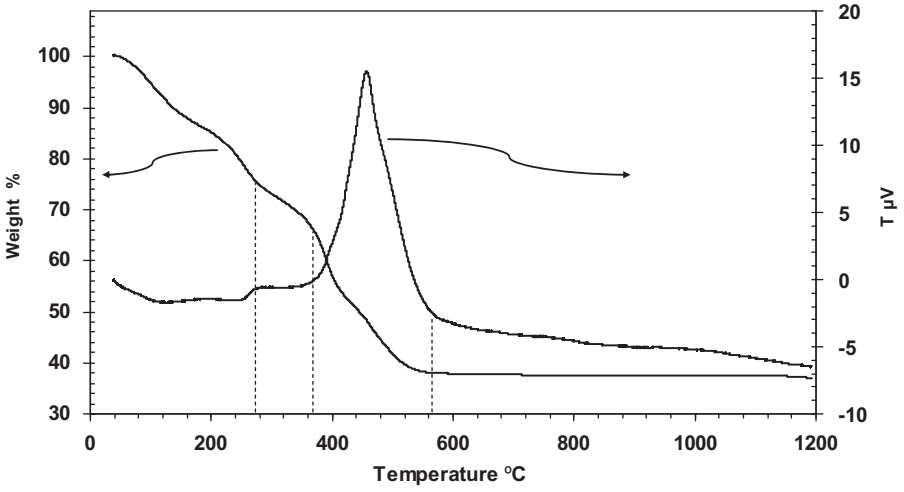

Fig. 1. STA curve (TG and DTA) of magnesium aluminum titanate precursor.

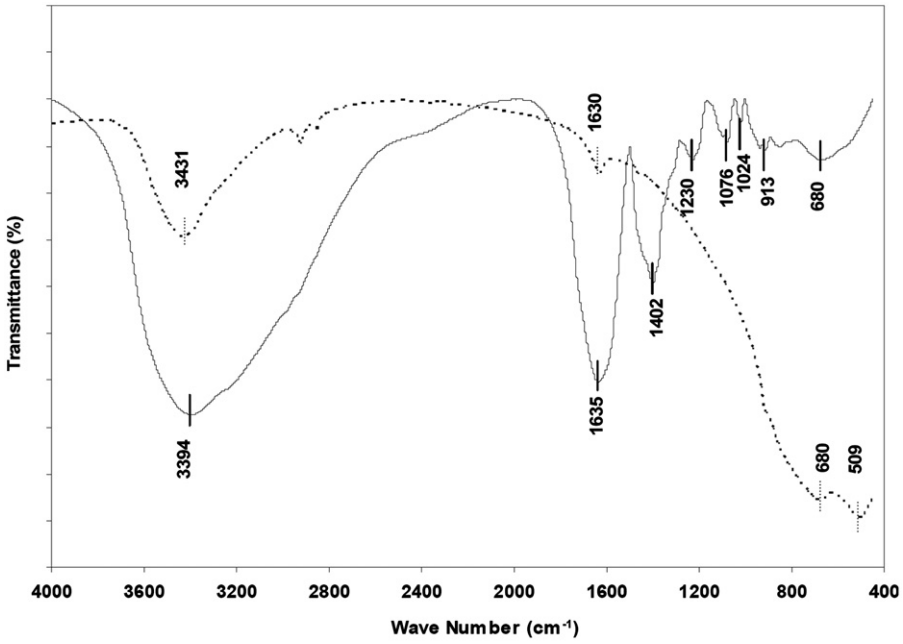

Fig. 2. FTIR spectra of dried gel at 120 °C (solid curve) and calcined gel at 800 °C (dashed curve).

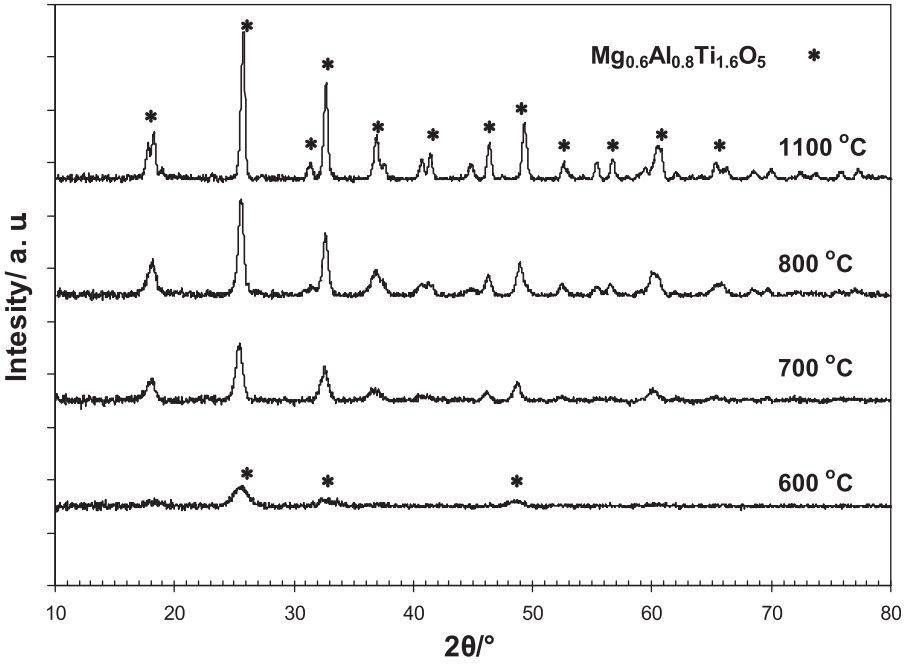

Fig. 3. X-ray diffraction patterns of calcined gel at different temperatures in an electric furnace.

M–O–M' vibration of crystalline structure that appears in the gel structure with a broad peak at 680 cm^{-1} [16].

X-ray diffraction patterns of samples with different calcination temperatures are shown in Fig. 3. This figure shows that the formation of crystalline $Mg_{0.6}Al_{0.8}Ti_{1.6}O_5$ phase starts at about 600 °C, immediately after burning the residual citric acid and ethanol in compounds intertwined prior with the metal cations by oxygen atoms as a binder in the gel structure.

Other peaks of the mono-phase magnesium aluminum titanate appeared as temperature increased to 1100 °C. The diffraction lines of $Mg_xAl_{2(1-x)}Ti_{(1+x)}O_5$ with $x=0.6$, (JCPDS card no. 34-1062) shifted to smaller angles in comparison with pure Al_2TiO_5 diffraction lines (JCPDS card no. 70-1435) due to substitution of two ions of Al^{3+} with Mg^{2+} and Ti^{4+} ions during solid solution formation [5]. Regarding Vegard's law and $MgTi_2O_5$ diffraction pattern (JCPDS card no. 20-0694), in the Al_2TiO_5 and

$MgTi_2O_5$ solid solutions system, the X-ray patterns of synthesized powder in this study are in agreement with $Mg_{0.6}Al_{0.8}Ti_{1.6}O_5$ diffraction lines [5,22]. Another reason for the left shifting of the peaks in X-ray spectra may be attributed to nanometric size of the crystallite produced by low temperature synthesis. Furthermore, there were no crystallizations of other superfluous phases such as alumina, rutile, $MgAl_2O_4$ or $MgTi_2O_5$ during the calcining processes that can be related to full homogeneity of precursor in atomic level in non-hydrolytic sol–gel [18]. With increasing temperature, the X-ray peak broadening decreased with the increase of crystallite size (Fig. 3). The phase stability of $Mg_{0.6}Al_{0.8}Ti_{1.6}O_5$ at 1100 °C can be associated with equilibrium constant, K, in the following reaction [4]:

$$Mg_xAl_{2(1-x)}Ti_{(1+x)}O_5 \rightarrow (1-x)MgAl_2O_4 + (2x-1)MgTi_2O_5 + 3(1-x)TiO_2 \quad (0.5 < x < 1) \qquad (8)$$

Buscaglia and Nanni reported that the decomposition temperature value, T_d=1067 °C, can be used as thermodynamic approach for decomposition reaction of aluminum titanate [4]. Moreover, the phase stability at low temperatures can be ascribed to kinetic stability of Al_2TiO_5–$MgTi_2O_5$ solid solutions. Some physical properties of synthesized powders are listed in Table 1. At the lowest calcination temperature, S1 sample has the maximum value of SSA (≈ 98.2 m^2/g) and minimum value of particle size (≈ 16.5 nm). It is obvious that the increase of calcination temperature brings about the increase of particle size and decrease of surface area.

Nitrogen adsorption/desorption isotherms of calcined powders at 600 °C (S1) and 700 °C (S2) are shown in Fig. 4. Porous materials are generally classified on the basis of pores diameters (r_p), into microporous ($r_p < 2$ nm), mesoporous (2 nm < r_p < 50 nm) and macroporous solids (50 nm < r_p) by the International Union of Pure and Applied Chemistry (IUPAC). Thereof both hysteresis loops are type IV, as classified by IUPAC, which is characteristic of mesoporous materials. Additionally, the two branches of the hysteresis loops are almost vertical and nearly parallel which is consistent with H1 hysteresis loops of the N_2 adsorption isotherms. It is a particular property of mesoporous materials with channel-like pores [23,24]. Shifting toward the high pressures is the main difference between S1 and S2 loops, indicating a significant increase in the pore size as a function of calcination temperature [25]. With

Table 1
Variation of specific surface area and particle size with calcination temperatures.

Sample	Calcination temperature (°C)	SSA (m^2/g)	D_{BET} (nm)	D_{XRD} (nm)
S1	600	98.2	16.5	7
S2	700	58.7	27.6	12
S3	800	–	–	27
S4	1100	–	–	37

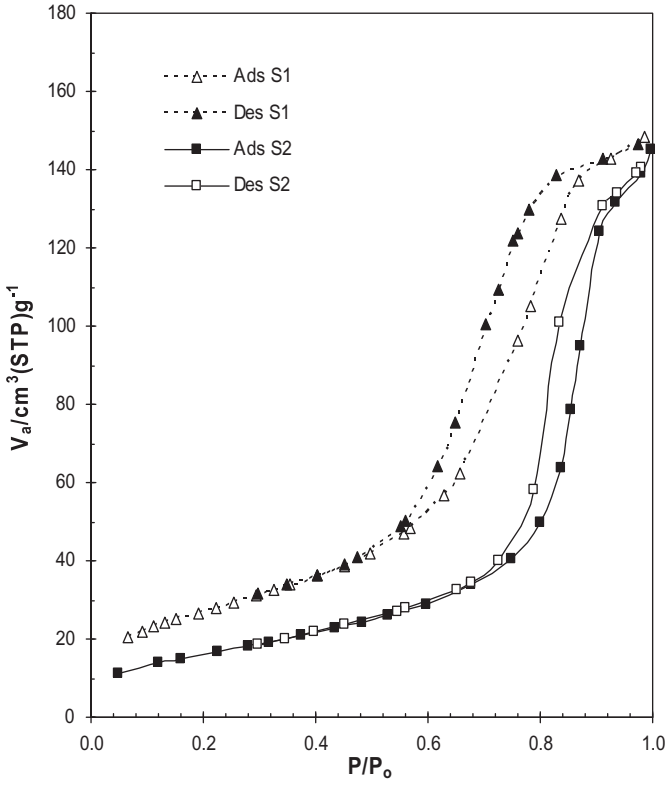

Fig. 4. Nitrogen adsorption/desorption isotherms of powders; S1 and S2 are related to calcination temperatures of 600 and 700 °C, respectively.

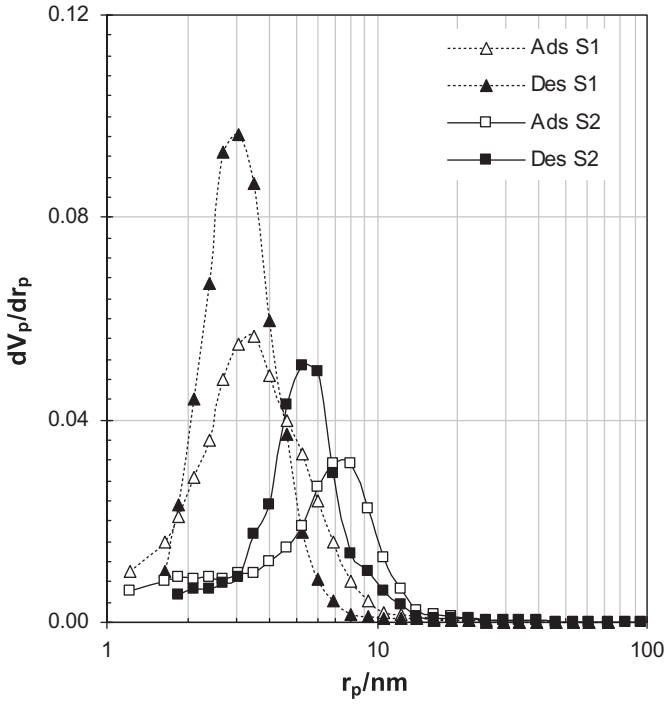

Fig. 5. Pore size distribution of calcined powders; S1 and S2 are related to calcination temperatures of 600 and 700 °C, respectively.

increasing calcination temperature from 600 to 700 °C, the size of the crystallized particles increased (Table 1) and consequently the pore size increased. The pore size distribution of

S1 and S2 powders (Fig. 5) was obtained from the nitrogen adsorption and desorption isotherms using the Barrett–Joyner–Halenda (BJH) method. The pore size increased from 3 nm (an average of adsorption and desorption maximum values) to 6 nm in agreement with the hysteresis loops.

SEM images of synthesized $Mg_{0.6}Al_{0.8}Ti_{1.6}O_5$ powders at different temperatures are illustrated in Fig. 6. Obviously, from samples S1 to S3, the increase in calcination temperature from 600 to 800 °C leads to the enhancement in the size of synthesized nano-particles. In sample S4, the extraordinary increment of particle size (larger than 500 nm) was observed at 1100 °C due to the localized sintering of nano-particles. Moreover, these particles have non-uniformity in their shape and size as a result of partial sintering. It is clear that the formation and growth of a crystalline structure from primary cationic and anionic mixed elements need diffusion of each element to the ordered crystal and diffusion phenomena demand time and temperature. While the structure of dried gel was formed from ordered component prior to aging, phase crystallization behavior due to surplus atoms (such as C, H, Cl and O) may be different from what occurs in diffusion phenomena in solid state reactions of oxides. After elimination of the extra atoms only the necessary Al^{3+}, Ti^{4+}, Mg^{2+} cations and O^{2-} anions will remain in a semi-amorphous network. With regard to the atomic level of homogeneity in the semi-amorphous network, the minimum distance of diffusion is required for the crystallization of $Mg_{0.6}Al_{0.8}Ti_{1.6}O_5$ phase. Therefore, it seems that the decomposition of gel and crystallization events take place simultaneously and released heat from organic components burning is sufficient for limited diffusion of ions.

4. Conclusions

Fabrication of aluminum titanate and magnesia solid solution compound via inorganic cations sources at low temperature is feasible. The maximum degree of atomic level homogeneity in the dried gel and presence of oxygen atoms as a network former are the main causes of the formation of $Mg_{0.6}Al_{0.8}Ti_{1.6}O_5$ at low temperature (600 °C).

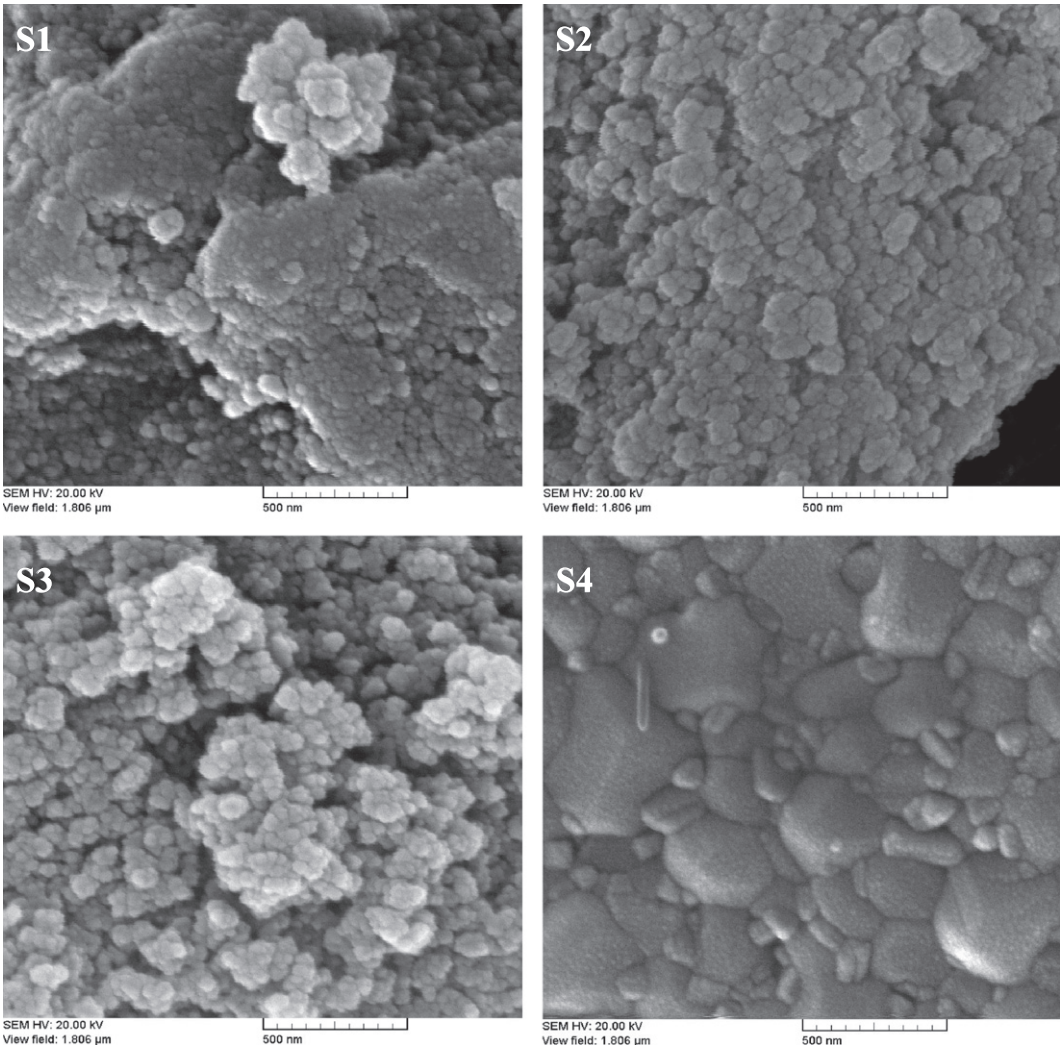

Fig. 6. SEM micrograph of S1, S2, S3 and S4 samples calcined in a furnace at 600, 700, 800, and 1100 °C, respectively.

The size of the primary nano-sized particles was a function of calcination temperature. The size of finest crystalline particles was 16.5 nm obtained at 600 °C. The decomposition of $Mg_{0.6}Al_{0.8}Ti_{1.6}O_5$ was not observed in the temperature range of 600–1100 °C due to its thermal stability in comparison with pure Al_2TiO_5.

References

[1] S. Ananthakumar, M. Jayasankar, K.G.K. Warrier, Microstructural, mechanical and thermal characterisation of sol–gel-derived aluminum titanate–mullite ceramic composites, Acta Materialia 54 (2006) 2965–2973.

[2] R.D. Skala, D. Li, I.M. Low, Diffraction, structure and phase stability studies on aluminum titanate, Journal of the European Ceramic Society 29 (2009) 67–75.

[3] J. Weihui, W. Hengyong, F. Guo, Z. Yanhua, Y. Yun, Effect of oxygen donor alcohols on low temperature non hydrolytic sol–gel synthesis of aluminum titanate, Journal of the Chinese Ceramic Society 36 (2008) 11–16.

[4] V. Buscaglia, P. Nanni, Decomposition of Al_2TiO_5 and $Al_{2(1-x)}Mg_x$-$Ti_{(1+x)}O_5$ ceramics, Journal of the American Ceramic Society 81 (1998) 2645–2653.

[5] Q. Shen, Y. Hu, C.B. Wang, M.Z. Li, L.M. Zhang, Effect of $MgTi_2O_5$ addition on thermal shock resistance of Al_2TiO_5, Key Engineering Materials 280–283 (2005) 1187–1190.

[6] H.R. Rezaie, R. Naghizadeh, N. Farrokhnia, S. Arabi, M. Sobhani, The effect of Fe_2O_3 addition on tialite formation, Ceramics International 35 (2009) 679–684.

[7] B. Freudenberg, A. Mocellin, Aluminum titanate formation by solid-state reaction of fine $A1_2O_3$ and TiO_2 powders, Journal of the American Ceramic Society 70 (1987) 33–38.

[8] H.L. Lee, J.Y. Jeong, H.M. Lee, Preparation of Al_2TiO_5 from alkoxides and the effects of additives on its properties, Journal of Materials Science 32 (1977) 5687–5695.

[9] A.M. Segadaes, M.R. Morelli, R.G.A. Kiminam, Combustion synthesis of aluminum titanate, Journal of the European Ceramic Society 18 (1998) 771–781.

[10] P. Oikonomou, Ch. Dedeloudis, C.J. Stournaras, Ch. Ftikos, Stabilized tialite–mullite composites with low thermal expansion and high strength for catalytic converters, Journal of the European **Ceramic** Society 27 (2007) 3475–3482.

[11] H.R. Rezaie, M. Sobhani, R. Naghizadeh, Formation and decomposition of sol–gel synthesized aluminum titanate nano powders at the presence of Fe_2O_3 additive, Defect and Diffusion Forum 273–276 (2008) 549–553.

[12] P. Innocenzi, A. Martucci, L. Armelao, Low temperature synthesis of $Mg_xAl_{2(1-x)}Ti_{(1+x)}O_5$ films by sol–gel processing, Journal of the European Ceramic Society 25 (2005) 3587–3591.

[13] M. Andrianainarivelo, R.J.P. Corriu, D. Leclercq, P.H. Mutin, A. Vioux, Nonhydrolytic sol–gel process: aluminum titanate gel, Chemistry of Materials 9 (1977) 1098–1102.

[14] M.L. Di Vona, R. Polini, P. Sebastianelli, S. Licoccia, A non-hydrolytic sol–gel approach for the preparation of $Mg_xAl_{2(1-x)}$-$Ti_{(1+x)}O_5$ powders, Journal of Sol–Gel Science and Technology 31 (2004) 95–98.

[15] M. Sobhani, H.R. Rezaie, R. Naghizadeh, Sol–gel synthesis of aluminum titanate (Al_2TiO_5) nano-particles, Journal of Materials Processing Technology 206 (2008) 282–285.

[16] M. Crisan, M. Zaharescu, A. Jitianu, D. Crisan, M. Preda, Sol–gel poly-component nano-sized oxide powders, Journal of Sol–Gel Science and Technology 19 (2000) 409–412.

[17] Y. Zhu, L. Zhang, C. Gao, L. Cao, The synthesis of nanosized TiO_2 powder using a sol–gel method with $TiCl_4$ as a precursor, Journal of Materials Science 35 (2000) 4049–4054.

[18] M. Andrianainarivelo, R.J.P. Corriu, D. Leclercq, P.H. Mutin, A. Vioux, Nonhydrolytic sol–gel process: aluminum and zirconium titanate gels, Journal of Sol–Gel Science and Technology 8 (1977) 89–93.

[19] G.P. Ricci, Z.N. Rocha, S. Nakagaki, K.A.D.F. Castro, A.E.M. Crotti, P.S. Calefi, E.J. Nassar, K.J. Ciuffi, Iron–alumina materials prepared by the non-hydrolytic sol–gel route: synthesis, characterization and application in hydrocarbons oxidation using hydrogen peroxide as oxidant, Applied Catalysis A: General 389 (2010) 147–154.

[20] R. Wahab, I.H. Hwangb, Y.S. Kima, J. Musarratc, M.A. Siddiquic, H.K. Seo, S.K. Tripathye, H.S. Shin, Non-hydrolytic synthesis and photo-catalytic studies of ZnO nanoparticles, Chemical Engineering Journal 175 (2011) 450–457.

[21] D.M. Ibrahim, A.A. Mostafa, T. Khalil, Preparation of tialite (aluminum titanate) via the urea formaldehyde polymeric route, Ceramics International 25 (1999) 697–704.

[22] Q.C. Zhang, Q.M. Ye, G. Li, J.H. Lin, J.F. Song, S.H. Chang, J. Liu, Effect of Mg doping level on properties of sol–gel tialite, Materials Letters 62 (2008) 832–836.

[23] K.S.W. Sing, Reporting physisorption data for gas/solid systems with special reference to the determination of surface area and porosity, Pure and Applied Chemistry 54 (1982) 2201–2218.

[24] L. Zhang, A. Bogershausen, H. Eckert, Mesoporous $AlPO_4$ glass from a simple aqueous sol–gel route, Journal of the American Ceramic Society 88 (2005) 897–902.

[25] S.M. Morris, J.A. Horton, M. Jaroniec, Soft-templating synthesis and properties of mesoporous alumina–titania, Microporous and Mesoporous Materials 128 (2010) 180–186.